Available online **www.ijpras.com**

International Journal of Pharmaceutical Research & Allied Sciences, 2017, 6(4):95-106

Research Article

ISSN : 2277-3657
CODEN(USA) : IJPRPM

Rheology, Morphology, Mechanical Properties and Cure Characterization of Rubber Nanocomposite based on NBR/SBR Blends Filled with Montmorillonite: Effect of Feeding Sequence

Mohammad Reza Mojahedi Jahromi*

Department of Polymer Engineering, Islamic Azad University, Science and Research Branch, Yazd, Iran.

ABSTRACT

In this work, nanocomposites based on acrylonitrilebutadiene rubber/styrene butadiene rubber (NBR/SBR) at 50 / 50 blend ratio with cloisite 15A(C15A) and cloisite 30B(C30B) nanoparticle using two feeding sequence technic including masterbatch (MB) and direct (D) technics were prepared via melt mixing method. In the first technic, the MB of C30B with NBR and C15A with SBR were prepared distinctly, and then, the secondary rubber was added. In the second technic, the nanocomposites were directly compounded by mixing NBR/SBR with nanoparticles. The effects of OC composition on the cure characteristics were studied, and according to the cure characteristics, both types of OC caused a reduction in the scorch time and optimum cure time of the nanocomposite compound. Morphology and rheological behavior of prepared nanocomposite were investigated using x- ray diffraction (XRD), rheometer mechanical spectroscopy (RMS) and scanning electronmicroscopy (SEM). Experimental Results demonstrated intercalation structure and better dispersion for 5 Phr montmorillonite of prepared nanocomposites by the first technic. Nanocomposites containing C30B caused better mechanical properties because of more interaction with the rubber chains. Nanocomposite which contains 10 phr of C30B by the second technic has the most dispersion, distribution and the exfoliation structure are observed.

Keywords: *styrene butadiene rubber (SBR); acrylo nitrile butadiene rubber (NBR); montmorillonite; nanocomposite; morphology; feeding sequence.*

---

1. INTRODUCTION

Blending the polymers offers novel material with tailored properties. Most polymer blend are thermodinamically immiscible which results in phase separation upon blending and weak properties [1-2]. Compatibilizers are demanded in order to overcome the weak interfacial adhesion resulting in inferior mechanical properties. Upon preparing polymer nanocomposites containing clay, whether miscible or immiscible, the clay has the inclination to play a compatibilizing role with these polymer blends. The high-efficiency polymeric materials are provided by the mentioned nanocomposites through making an integration of contributing polymers' advantages. When two immiscible polymers are blended during melt extrusion, one phase is mechanically dispersed (droplets) inside the other. The size and shape of the dispersed phase depends on many processing parameters involving rheology, interfacial properties, and the composition of the blend. Distribution of OCs at the interface results in coalescence suppression of droplets and reduction of interfacial tension [3-4-5]. A number of researchers have carried out compatibilizing of immiscible polymer blends by copolymers [1-6-7-8]. For instance, Botros et al. investigated the effect of using poly glycidyl methacrylate-g-butadiene (PGMA-g-BR) on homogeneity of SBR/NBR blends and reported that no phase separation

took place, indicating a change of morphology and enhancement of the homogeneity of the SBR/NBR blend. Compatibilization of polymer blends using inorganics nanoparticles have been studied [9-10-11-12-13]. Li et al. investigated the effect of silica nanoparticles on the partially miscible polymer blend PMMA/SAN and reported that the hydrophobic silica nanoparticles were localized at the PMMA/SAN interface, and the inhibition of coalescence corresponded to the presence of a solid barrier (the nanoparticles) between the polymers prevented the coarsening process [9].

Moreover, using mineral clay in immiscible polymer blends was investigated [14-15-16]. Abreu studied the effect of clay mineral addition to bio-based blends on morphology and physical properties of thermoplastic starch (TPS) and polypropylene grafted with maleic anhydride (PP-g-MA) and showed a very good dispersion of the clay mineral in the polymer matrix, an increase of polymer compatibility and an improvement in mechanical properties [16]. For improving the clay mineral compatibility with the hydrocarbon matrices, the hydrophilic clay mineral is modified with various alkyl ammonium salts to expand the interlayer space as well as reduce the surface energy of the layers [2]. The preparation of SBR/NBR blends are challenging due to their poor compatibility and unfavorable interaction between SBR and NBR [2-18]. The present paper is concerned with application of OC (C15A, C30B) as a compatibilizer for SBR/NBR blend. Recently, Monfared et al. studied immiscible acrylonitrile butadiene rubber/styrene butadiene rubber (NBR/SBR) blends and their nanocomposites with C15A and C30B nanoparticles which were prepared via a melt mixing method. The experimental results proved that the C30B, the more hydrophilic OC, tended to confine in the NBR, the more polar rubber phase, and in the interface, whereas in C15A, the less hydrophilic one was located at the SBR and interface [2-17]. In the above research, several compositions of SBR/NBR with C15A and C30B were prepared except 50/50, and feeding sequence was not discussed. In our study, both masterbatch and direct technic were used in preparation of SBR/NBR nanocompsite via melt mixing. Morphology of the blend and rheological behavior and mechanical properties through making use of X-ray diffraction (XRD), melt rheo mechanical spectroscopy (RMS), scanning electron microscopy (SEM), and tensile test were investigated.

2. Experiments

2-1 MATERIALS

SBR (1502) with a styrene content of 23.5%, a density of 0.94 g/cm^3, and Mooney viscosity of 51/5 [M_L (1+4) 100c^o] was supplied by EmamPetro Chemical Co (Iran). NBR (6240) with an acrylonitrile content of 34%, a density of 0.97g/cm^3 and Mooney viscosity of 45[M_L (1+4) 100c^o] was purchased from LCCo (Korea), respectively. OCC15A and C30B (OC) were obtained by Southern Clay Products (USA). They are natural monmorillonite which have been modified with bis(2-hydroxy-ethyl) methyl tallow quaternary ammonium with a cation exchange capacity of 90 mequiv/100 g and dimethyl-dihydrogenated tallow ammonium with a cation exchange capacity of 125 mequiv/100 g. The curing system, including merkaptobenzo-thiazole-Disulfide, zinc oxide, stearic acid and sulfur were supplied by Yazd Tires (Iran).

2-2 Preparation of nanocomposites

Nanocomposite samples containing 50/50 blend ratio of NBR/SBR with and without OC using two feeding sequence technics including both masterbatch and direct technic were prepared via melt mixing method in an internal Mixerat a temperature of 60^{o}C and a rotor speed of 80 rpm for 20 min. The formulation of the compounds (Table 1) for the MB technic (the first technic) is given by the name XY-Z in which X shows the SBR or NBR, Y shows the kind and used amount of cloisite (for instance, Y=B10 points out to 10 phr C30B and A10 points out to 10 phr C15A) and Z shows SBR or NBR again and also for direct technic is XZ-Y. Then, omenclature is as follows: N, S, B, A stand for NBR, SBR, C30B and C15A, respectively. As an example, NB5-S indicates that SBR is mixed with MB compound containing 5 phr of C30B and NBR at 50 / 50 blend ratio (NBR/SBR). Also, SN-B5 point out 5 phr of C30B was directly mixed with SBR/NBR compound. Then, the curing agent was added on a two roll millat at temperature of 50^{o}C for 5min. The samples were cured at a temperature of 150^{o}C with respect to their cure characteristics obtained by rheometric technic. The curing process was carried out at a pressure of 100 bars in a hot press molding.

Table 1. Samples code and composition.

Sample code MB	D	NBR/SBR	C15A	C30B
	S-N		-	-
SA5-N	SN-A5		5	-
SA10-N	SN-A10	50/50	10	-
NB5-S	SN-B5		-	5
NB10-S	SN-B10		-	10

3. Characterization

The cure characteristics were studied using Rheometer (Hiva900, ASTM D5289). The X-ray diffraction analysis for OC and nanocomposites were carried out using a Philips model X'Pert (Netherlands), X-ray diffractometer with Ni-filtered CoK_{α} radiation (λ=1/540598Å) at 40Kv and 30 mA in low angle to study dispersion of the OC in the nanocomposites at room temperature.

The inter layer spacing of silicate layers was approximated using Bragg's law, $d=\lambda/2\sin\theta max$. The samples were scanned in the 2θ range from 1 to 12° at a rate of $0.02^{\circ}\ S^{-1}$.

Rheological behavior of nanocomposites was studied using rheometric mechanical spectrometer Antonpaar, MCR300 (Austria) with parallel plate (diameter of 43mm) at a temperature of 160ºC, strain amplitude of 1%, and frequency range of 0.01-600 Hz.

The morphology of samples was freeze-fractured in liquid nitrogen, covered with a thin layer of gold prior to observation; using a scanning electron microscope (SEM), EM3200 Model (kykyCo, China) operated at 30kv. Tensile properties of the molded samples were carried out according to ASTM 412-29 using Hiwa machine at a cross head speed of 500 mm/min. In this study, a dumbbell shape was made of sample with a thickness of about 2 mm and was closed between the two jaws of tensile machine. In this section, temperature conditions and tensile rate were also constant. It should be noted that in order to reduce the error for each sample, five dumbbell shapes were made and tensile testing was investigated.

4. RESULTS AND DISCUSSIONS

4.1. XRD analysis

Fig. 1 shows the XRD patterns of the C15A, C30B and nanocomposites containing 5 phr of OC. The peak positions and interlayer spaces of prepared nanocomposites and increment amount of space with respect to OC are summarized in Table 2. It is indicated that the interlayer space of C30B, 1.657 nm, is increased to 5.251nm and 4.875nm for NB5-S and SN-B5 respectively. Also, SA5-N and SN-A5 samples represent the interlayer spacings 3.865 and 3.731 nm is an increase equal to 0.645 and 0.511 in interlayer space of C15A respectively. The peak (001) has mostly shifted to the left side, which can be attributed to greater dispersion of C30B than C15A. Also, the peak intensity in the nanocomposites containing C30B is lower, indicating that the nanocomposite structure has an interlayer structure and that it has probably been composed of the exfoliation structure.

This can be due to the greater polarity of the C30B and formation of the hydrogen bonding between Acrylo Nitrile groups in NBR phases and the Amonium salt modifier available on the OC surface. Fig. 2 shows the XRD patterns of the aforementioned OCs and nanocomposites containing 10 phr OC.

The characteristic peak (001) of NB10-S and SN-B10 demonstrates the interlayer Spacings of 4.293 and 3.451 nm.

Table 2.XRD analysis for prepared nanocomposite and OC.

Sample code	d(nm)	2θ	Δd
C30B	1.657	5.327	-
C15A	3.22	2.734	-
SA5-N	3.865	2.284	0.645
SN-A5	3.731	2.367	0.511
SA10-N	3.766	2.344	0.546
SN-A10	3.777	2.337	0.557
NB5-S	5.251	1.753	0.594
SN-B5	4.875	1.81	3.218
NB10-S	4.295	2.05	2.638
SN-B10	5.451	1.70	3.794

Increment of inter layer spacing with respect to C15A for SA10-N and SN-A10 is equal to 0.546 and 0.557; therefore, C30B has greater dispersion than C15A in rubber nanocomposite containing 5 and 10 phr of OC.

In the samples containing C30B, intensity of the main characteristic peak of them are lower, indicating the intercalation and partial exfoliation structure.

Moreover, according to Fig. 1 (Table 2) SA5-N with respect to SN-A5 has greater interlayer spacing. In other words, by adding C15A to the SBR, preparing the nanocomposite SBR/OC MB and then adding NBR, the nanoclay interlayer spacing will be increased, as compared with the second feeding sequence technic in which the nanoclay is added to the blend of rubbers. This can result from the polarity adaptation of this OC to the SBR rubber, as compared to the NBR rubber. It is suggested that the second peak appears due to the collapse of the layers of the OC and agglomeration of the nanoparticles [28].

As can be observed, the characterize peak (001) of the samples SA10-N and SN-A10 are at $2\theta=2.344^{o}$ and 2.337^{o}, respectively, showing the interlayer spacing of 3.766 and 3.777 nm (Fig 2, Table 2).

Also, the characteristic peak (001) of the two samples are approximately similar but the intensity of peak's SN-A10 is greater than SA10-N, indicating the greater agglomeration of the silicate layers in elastomer matrix.

Also, the peaks of NB5-S and SN-B5 have shifted to lower angles than OC, indicating the nanocomposite interlayer structure. The main characteristic peak of NB5-S is located at $2\theta=1.75^{0}$, demonstrating the interlayer spacing of 5.251 nm, while SN-B5, 4.875, prepared nanocomposite by the first technic, has greater interlayer spacing. In other words, due to the greater polarity of the NBR than that of SBR and its adaptation to C30B, by adding C30B to the NBR and then mixing with SBR, the interlayer spacing has been increased. Also interlayer space of SN-B10 (Table 2), is 5.451nm, while, for NB10-S, it is 4.293. On the other hand, by adding C30B to NBR to prepare MB and then adding SBR (MB technic) which causes more intercalation of NBR (more polarity) in to the C30B, it can be said that hard diffusion of C30B into SBR phase is the cause of interlayer space decrement for NB10-s.

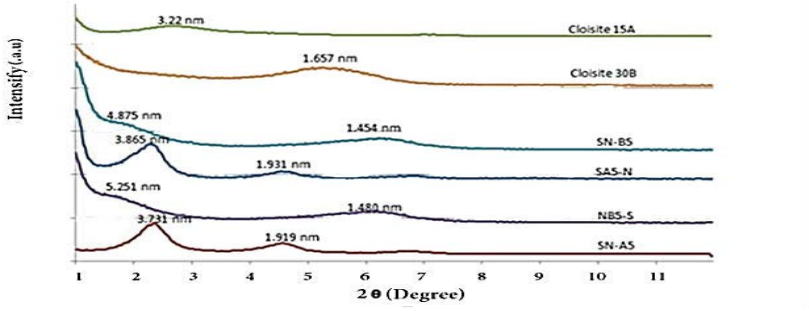

Fig. 1. XRD patterns of Cloisite15A, Cloisite 30B and samples containing 5 phr organoclay with different sequence feeding.

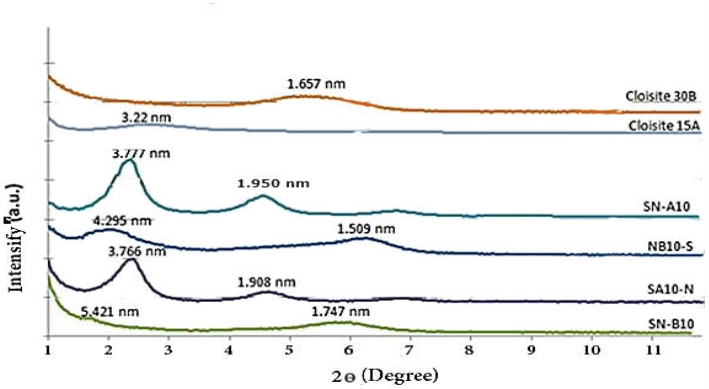

Fig. 2. XRD patterns of Cloisite15A, Cloisite 30B and samples containing 10 phr organoclay with different sequence feeding.

4.2. Rheological behavior

Rheological behavior (melt viscoelastic behavior) of foregoing nanocomposite containing 5 phr OC and that lacking OC (S-N) are shown in Fig. 3. Complex viscosity and shear storage modulus (G') of the nanocomposites filled with C30B (NB5-S, SN-B5) is higher than those filled with C15A (SA5-N, SN-A5) at all frequency regions. Storage modulus is independent of frequency at low frequency, it could be indicated as non-terminal behavior.

More complex viscosity and higher shear storage modulus of the nanocomposite in comparison to neat blend (S-N) are observed at all frequencies. By distributing and dispersing the nanoparticles in rubber matrix, the complex viscosity and shear storage modulus increase.

The melt viscoelastic behavior of the nanocomposite filled with 10 phr of OC (SN-B10, NB10-S, SN-A10, SA10-N) and that neat blend (S-N) are shown in Fig. 4, which indicate the stronger structure of nanocompsites containing C30B, due to the steep slopes at low frequency which lead to create the OC network.

The melt viscoelastic behavior of samples filled with 5phr of C15A (SA5-N and SN-A5) in the form of two different feeding sequences (MB and D technic) and the pure blend (S-N) are compared in Fig. 3, and indicates (at low frequency) that the elasticity of SA5-N nanocomposite is higher than that of SN-A5(fig5). In the first step, when 5 phr of C15A is added to SBR, due to great affinity between SBR and C15A and high mooney viscosity of rubber, nanoparticles were dispersed and distributed more and more which leads to be smaller of phase domains (droplet) of NBR. It is notable that, there is no significant difference between complex viscosity and shear storage modulus of samples. Also, higher complex viscosity and shear storage modulus of SN-A10 compared with SA10-N in low frequency about 0.01 (1/s) indicate greater distribution of OC in matrix, and domains of dispersed phase is smaller for SN-A10 (Fig. 4). More (elasticity) complex viscosity and higher shear storage modulus of NB5-S in comparison to SN-B5 (Fig. 3.5) in all frequency regions can be related to more intercalation of the NBR chains in the C30B interlayer space due to more affinity between NBR and C30B and greater distribution of OC leads to be smaller of phase domain of SBR component. Fig. 4 shows melt viscoelastic properties of NB10-S, SN-B10 and neat S-N. It demonstrates higher shear storage modulus and complex viscosity of SN-B10 which indicates better nanoparticle distribution and more intergallery space and OC network formation and exfoliation structure. The properties of melt viscoelastic of nanocomposites filled with C15A prepared using different feeding sequence (SA5-N, SN- A5, SA10-N and SN-A10) were evaluated in various frequencies particularly in low frequencies. As it is observed, these samples are equal regarding complex viscosity and shear storage modulus in approximately all ranges of frequencies, and the curves are superimposed on each other which reveal approximate equal distribution of OC and similar structural ability. In this respect, complex viscosity and shear storage modulus are more in SA5-N nanocomposite.

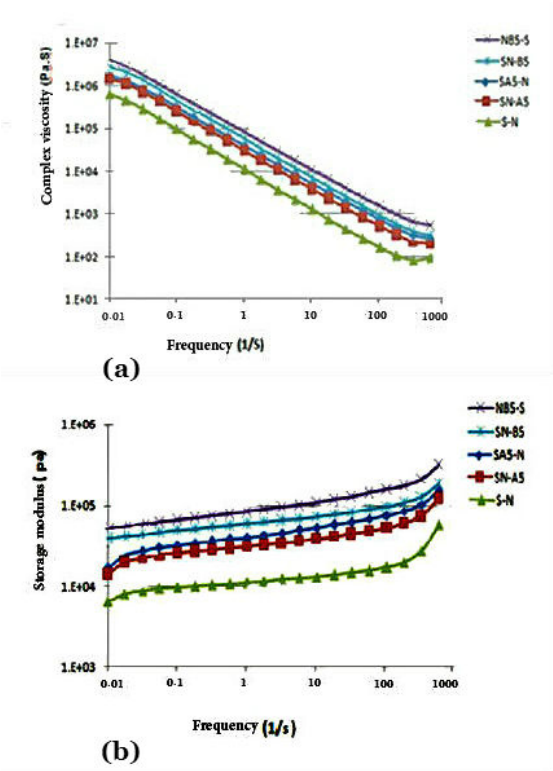

Fig.3. Complex viscosity (a), Storage modulus (b), of SBR/NBR/OC with 5 phr organoclay and pure blend.

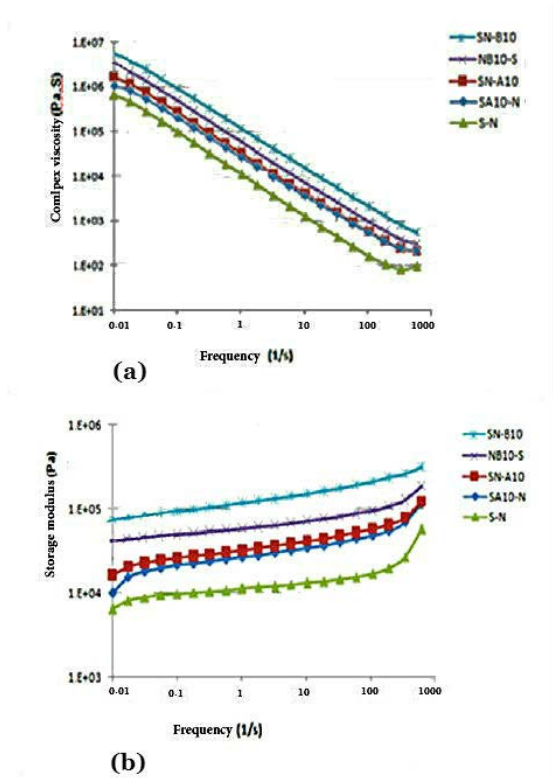

Fig. 4. Complex viscosity (a), Storage modulus (b), of SBR/NBR/OC with 10 phr organoclay and pure blend.

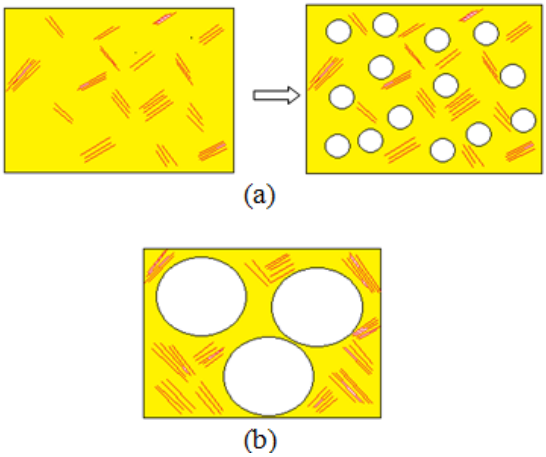

Fig.5. The storage modulus of the SBR/NBR (50/50) blend filled with 5 phr of OC using MB technic (a) and D technic (b) and its nanocomposites with a schematic depicting morphology of them.

4.3. SEM analysis

SEM micrographs of fractured surfaces of S-N, SA5-N and SN-A5 compounds containing 5 phr C15A are shown in Fig. 6. The rough fractured surface of SA5-N and SN-A5 (Fig. 6, b, c) compared with S-N (Fig. 6a) demonstrates interactions between the matrix and nanoparticles, implying the effective intercalation of SBR chains into the C15A interlayer spaces evidenced by the XRD patterns, while the fractured surface of neat S-N seems to be smoother. Fractured surface of SA5-N nanocomposite is slightly rougher than SN-A5, which indicates more interaction and brittle fracture behavior. Micrographs of fractured surfaces of SA10-N, SN-A10 and S-N are shown in Fig. 7. The unevenness fracture surface of nanocomposite samples (Fig7.b.c) compared with the samples lacking OC (S-N) reveals interaction between matrix and nanoparticles which shows interlayer structure and polymer chain penetration into silicate nanolayers which is confirmed by XRD pattern, while the fractured surface of elastomer sample seems smoother. The fractured surface of nanocomposite sample SN-A10 seems to be more uneven compared with SA10-N sample, which indicates more interaction between OC and rubber matrix and more interphase adhesion among blend components by comparing the roughness of the images of NB5-S, SN-B5 and S-N. Fig. 8 showed the presence of C30B in the NB5-S, Fig. (8b) resulted in better interaction between constituent components of this blend with respect to that of SN-B5 compound and enhancing interfacial adhesion, which is confirmed by XRD pattern and RMS. Fig. 9 shows images of fractured surfaces of SN-B10, NB10-S and S-N. Roughness of fractured surface of SN-B10 with respect to NB10-S indicates more interaction and better adhesion between the phases of SN-B10 compound.

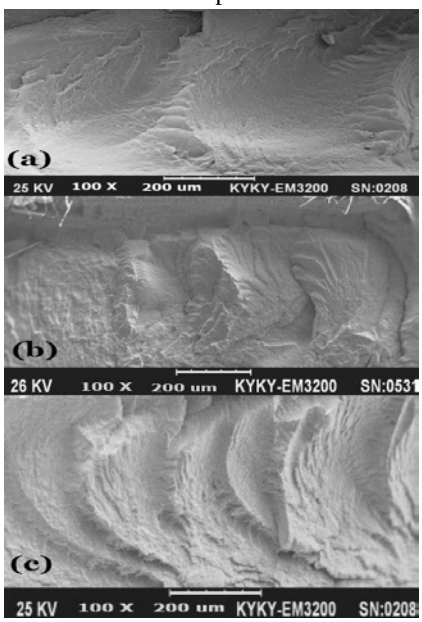

Fig. 6. SEM micrographs of (a) S-N unfilled elastomer blend and (b) SA5-N (C) SN-A5.

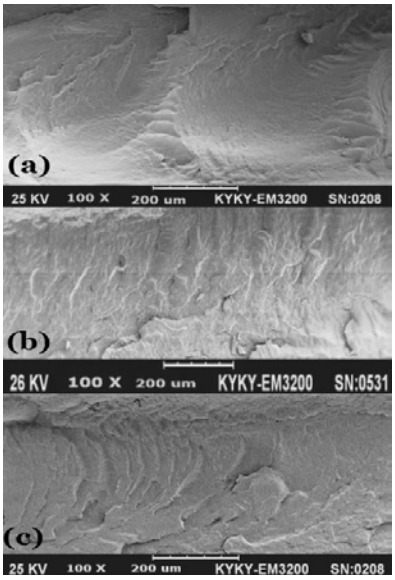

Fig. 7. SEM micrographs of (a) S-N unfilled elastomer blend and (b) SA10-N (C) SN-A10.

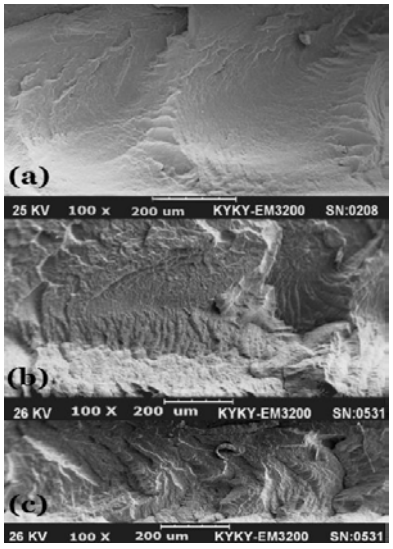

Fig. 8. SEM micrographs of (a) S-N unfilled elastomer blend and (b) NB5-S (C) SN-B5.

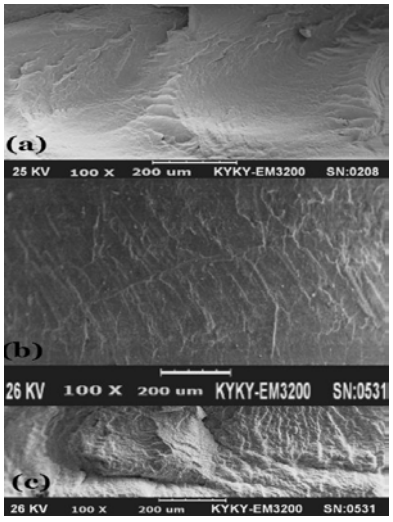

Fig.9. SEM micrographs of (a) S-N unfilled elastomer blend and (b) NB10-S (C) SN-B10.

4. 4. Cure characteristics

Cure characteristics, such as optimum cure time (Tc_{90}), scorch time (Ts_2), cure rate index (CRI) and torque differences (M_H-M_L) of nanocomposites prepared using different feeding sequence and containing various types and amounts of C15A and C30B are shown and compared in Table 3. The highest scorch time and optimum cure time refer to S-N blend; adding OC to rubber blend regardless of the feeding sequence leads to scorch time and optimum cure time reduction. In fact, functional amine groups of organic cations extracted from interlayer space of OC, which forms coordination complexes with ZnO and sulfur [18-20], causes facilitation in sulfur element and cure reaction of rubber distribution [21, 22].

Comparison between scorch time and cure time of the compound containing modified C15A and C30B shows that the scorch time and cure time will be lower in the blend percentage of SBR/NBR in the compounds containing C15A. It could be considered that higher scorch time and cure time in the compounds containing C30B is attributed to the presence of modified OH in C30B. It seems that OH groups available in C30B modifying structure play a retardant role compared with C15A. Also, evaluation of the cure rate index of such compounds shows that samples containing C15A reveals higher cure rate than the samples containing C30B. The maximum torque of the compounds prepared by two SBR/NBR rubbers with 50/50 percentage combination containing two types of C15A and C30B shows that in such combination, having homogeneous rubber phase will increase compared with the sample lacking nanoclay. That is while, no significant change has been observed in the minimum torque of samples.

Besides, regarding crosslink density, an indirect relationship is shown in torque difference and consequently, such behavior has been observed in the evaluation of the crosslink density. In other words, an increase is seen in the crosslink density at 50 / 50 blend ratio of SBR/NBR containing C30B, and sequence feeding does not influence the cure characteristics.

Zn, sulfur and functional modifying amine groups facilitate crosslink formation which shows increase in crosslink density [23, 24]. On the contrary, cure factors with low molecular weight in the interlayer space of OC provide increasing possibility of crosslink reaction of rubber chains in the interlayer of OC [25].

Table 3.Cure characteristics

Sample code	**Ts_2 (min:sec)**	**Tc_{90} (min:sec)**	**M_H (dN.m)**	**M_L (dN.m)**	CRI (min^{-1})
S-N	3:01	13:48	10.553	1.242	9.55
SA5-N	3:15	11:30	12.277	1.242	12.26
SN-A5	3:17	11:37	12.829	1.242	12.19
SA10-N	3:30	12:43	12.414	1.379	10.95
SN-A10	3:25	12:48	12.415	1.379	10.83
NB5-S	3:29	13:47	15.174	1.242	9.82
SN-B5	3:18	13:45	14.485	1.242	9.73
NB10-S	3:43	14:08	15.174	1.379	9.38
SN-B10	3:38	14:39	15.175	1.379	9.08

4.5. Mechanical properties

Tensile strength, elongation at break, and stress at 100% of elongation of prepared nanocomposites are presented in Fig. 10-12. The tensile strength of SBR/NBR blend containing 5 phr of C15A prepared via master batch technic is higher than that of direct technic because of better dispersion and interfacial adhesion of C15A in rubber matrix. Also, tensile strength of the nanocomposite filled with 5 phr of C30B shows similar result as the above mentioned. But the increase in OC content from 5 to 10 phr in rubber blend of SBR/NBR requires using second technic of feeding sequence. Tensile strength of nanocomposite prepared via the direct technic increases with respect to master batch technic.

As it can be observed, mechanical properties of nanocomposites containing C30B are higher than those containing C15A. Fig.11. shows elongation at break along with increase in tensile strength in above mentioned samples due to OC surface slipping if stress. Stress at 100% elongation of nanocomposites filled with 5 phr of OC prepared via master batch technic and 10 phr of OC prepared using direct technic is higher (Fig. 12) which will be considered as a criterion for filled rubber hardness. Mechanical properties of SBR/NBR blend without OC in comparison to nanocomposites at tensile strength, elongation at break and stress at 100% elongation are weaker. This result is due to the ability of compatibility and strengthening of OC in the nanocomposites, and also reveals the higher hardness of nanocomposite. It is notable that evaluation of the mechanical properties of nanocomposites from the aspect of type of added OC effect shows that tensile strength, elongation at break and stress at 100% elongation of the samples containing C30B are higher which agrees with micro-structural point of view. The nanocomposite containing 10phr of C30B prepared using the second technic (adding OC to the mixture of rubbers, (SN-B10)) from aspect of micro structure and mechanical properties is the best which can be attributed to the most distribution and interaction of OC in rubber matrix. All results are consistent.

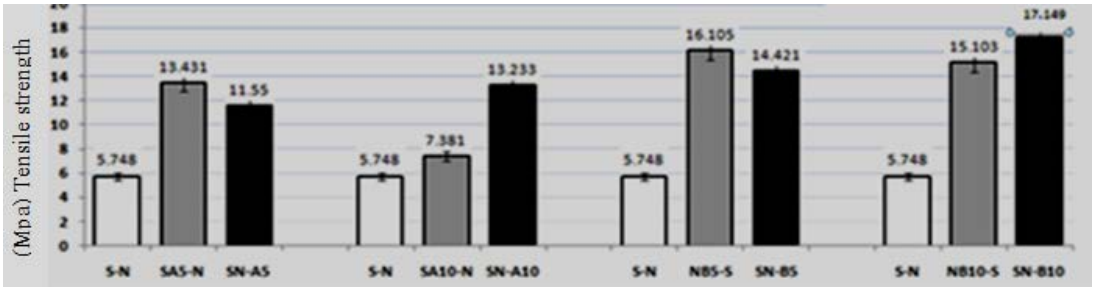

Fig. 10. Tensile strength of SBR/NBR/OC with 5 phr,10 phr modified nanoclay with different feeding sequences.

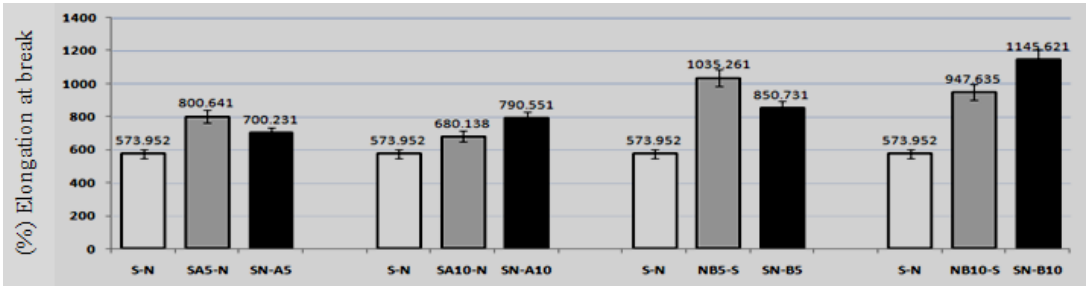

Fig. 11. Elongation at break of SBR/NBR/OC with 5 phr, 10 phr modified nanoclay with different feeding sequences.

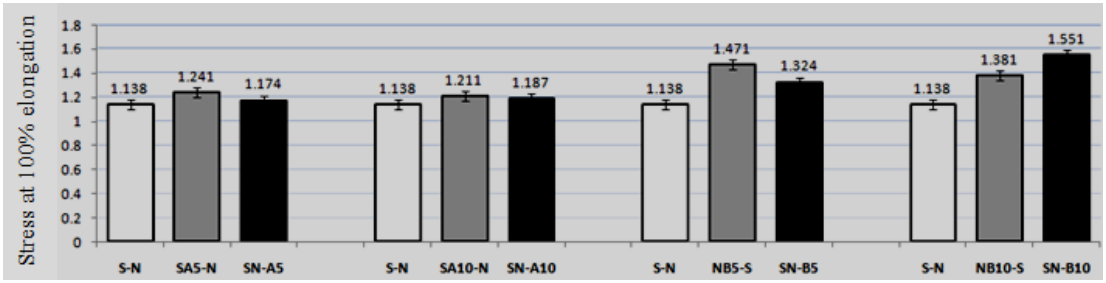

Fig. 12. Stress at 100% elongation of SBR/NBR/OC with 5 phr, 10 phr with different feeding sequences and unfilled blend.

5. CONCLUSION

In order to investigate the effect of amounts and types of OC and feeding sequence on the curing characteristics, morphology, and mechanical properties of rubber blend (NBR/SBR) at the ratio of 50/50, two types of OC, namely C15A and C30B were selected and the nanocomposites were prepared. Also, two technics of feeding sequence were utilized. The first technic was adding the modified OC to one of the two rubbers in order to prepare the MB. Then the second rubber was added. The second technic was adding OC to the rubber blend directly.

Cure characteristics using Rheometer results lead to an increase in the cure rate index and a decrease in scorch time and optimum cure time.

In this research, after investigating the obtained results from the XRD, RMS, SEM and tensile tests, it was observed that the peak (001) of the X-ray diffraction of the nanocomposite SBR/NBR/OC shifted to lower angles, as compared to the characteristic peak (001) of OC.

This demonstrates the intercalation structure of filled blend. The obtained results of tests revealed better properties of nanocomposites containing C30B compared with those containing C15A, regardless of the feeding sequence. It can be stated that regardless of the OC type, by increasing the amount of OC, the second technic (direct technic) is preferable. Finally, the key factor in the desirable OC dispersion in the blend matrix of SBR /NBR (with different polarities) is the OC polarity.

ACKNOWLEDGEMENTS

The Atomic Energy Organization of Yazd (Radiotherapy Center of Yazd) is greatly appreciated for its assistants and we are thankful to others providing comments that greatly improved the manuscript.

REFERENCES

1. Ramesan, M.T., Premalatha, C.K., Alex. R., 2001. Influence of carbon black on uncompatibilised and compatibilised SBR–NBR blends. J. Plastics, Rubber and Composites Macromolecular Engineering. 30, 355-362.

2. Monfared, A., Jalali-Arani, A., 2015. Morphology and rheology of (styrene buta diene rubber/acrylonitrile-butadiene rubber) blends filled with organoclay: The effect of nanoparticle localization. J. Clay Science. 108, 1-11.

3. Essawy, H.A., Khalil, A.M., Tawfik, M.E., 2014. Compatibilization of NBR/SBR blends using amphiphilic montmorillonites: A dynamic mechanical thermal study. J. Elastomers & plastics. 46, 1-13.

4. Sundararaj, U., Macosko, CW., 1995. Drop breakup and coalescence in polymer blends: the effects of concentration and compatibilization. J. Macromolecules. 28, 2647-2657.

5. Hajibaba, A., Masoomi, M., Nazockdast, H., 2015. The role of hydrophilic organoclay in morphology development of poly (butylene terephthalate)/polypropylene blends. J. High Performance Polymers. 28, 85-95.

6. Botros, S.H., Moustafa, A.F., Ibrahim, S. A., 2006. Improvement of the Homogeneity of SBR/NBR Blends using Polyglycidylmethacrylate-g-Butadiene Rubber. J. Applied Polymer Science. 99, 1559- 1567.

7. Khalf, A. I., Nashar, D.E.El., Maziad, N. A., 2010. Effect of grafting cellulose acetate and methylmethacrylate as compatibilizer onto NBR/SBR blends. J. Materials and Design. 31, 2592-2598.

8. Noriman, N. Z., Ismail, H., Rashid, A.A., 2010. Characterization of styrene butadiene rubber/recycled acrylonitrile-butadiene rubber (SBR/NBRr) blends: The effects of epoxidized natural rubber (ENR-50) as a compatibilizer. J. Polymer Testing. 29, 200-208.

9. Li, W., 2011. Effect of silica nanoparticles on the morphology of polymer blends. Technische Universiteit Eindhoven. 1-159.

10. Wang. H., Zeng, C., Elkovitch, M., Lee, L.J., Koelling, K.W., 2001. Processing and properties of polymeric nano-composites. Polym. Eng. Sci. 41, 2036–2046.

11. Steinmann, S., Gronski,W., Friedrich, C., 2002. Influence of selective filling on rheological properties and phase inversion of two-phase polymer blends. Polymer 43, 4467–4477.

12. Gu, S. Y., Ren, J., Wang, Q. F., 2004. Rheology of polypropylene/clay nanocomposites. J. Appl. Polym. Sci. 91, 2427–2434.

13. Elias, L., Fenouillot, F., Majeste, J.C., Cassagnau, Ph., 2007. Morphology and rheology of immiscible polymer blends filled with silica nanoparticles. Polymer. 48 (20), 6029–6040.

14. Bergaya, F., Lagaly, G., 2013. Handbook of clay science. In: Bergaya, F., Lagaly, G. (Eds.), General Introduction: Clays, Clay Minerals, and Clay Science. Elsevier Ltd., Amsterdam. 2–20.

15. Bergaya, F., Jaber, M., Lambert, J. F., 2011. Clays and clay minerals. In: Galimberti, M. (Ed.), Rubber-Clay Nanocomposites. Science, Technology and Applications. John Wiley & Sons, Inc., New Jersey, 3–86.

16. Abreu, A. S., Oliveira, M., Machado, A. V., 2015. Effect of clay mineral addition on properties of bio-based polymer blends. J. Applied Clay Science. 104, 277- 285.
17. Monfared, A.R., Jalali Arani, A., Mohammadi, N., 2014. The Effect of Epoxidized Natural Rubber and two Kinds of Organoclay upon Molecular Interaction, Structure and Mechanical Properties of (Styrene-Butadiene Rubber/Acrylonitrile- Butadiene Rubber/Organoclay) Nanocomposites. J. Macromolecular Science. 53, 918-930.
18. Perez, L. D., Lopez, B. L., 2012. Thermal characterization of SBR/NBR blends reinforced with a mesoporous silica. J. Applied Polymer Science. 125, 327-333.
19. Varghese, S., Karger-Kocsis, J., 2003. Natural rubber-based nanocomposites by latex compounding with layered silicates. J. Polymer. 44, 4921-4927.
20. Varghese, S., Karger-Kocsis, J., 2004. Melt-compounded natural rubber nanocomposites with pristine and organophilic layered silicates of natural and synthetic origin. J. Polym. 91, 813-819.
21. Zheng, H., Zhang, Y., Peng, Z. L., Zhang, Y.X., 2004. Influence of clay modification on the structure and mechanical properties of EPD/montmorillonite nanocomposites. J. Polymer. 23, 217-223.
22. Krejsa, M.R., Koenig, J.L. The Nature of Sulfur Vulcanization in Elastomer Technology Handbook, CRC Press: Boca Raton,1993.
23. Zaborski, M.; Donnet, J.B. Macromol., 2003. Activity of fillers in elastomer network of different structure. Mcromol Symp. 194, 87- 100.
24. Mousa, A.; Karger-Kocsis, J., 2001. Rheological and thermodynamical behavior of styrene/butadiene rubber-organo clay nanocomposites. Macromol. Mater.Eng. 286, 260- 266.
25. LeBaron, P.C.; Wang, Z.; Pinnavaia, T. J.Appl. Clay Sci. 1999, 15, 11- 29.
27. Wang, Y., Zhang, L., Tang, C., 2000. Preparation and characterization of rubber-clay nanocomposites. J. Applied Polymer Science. 78, 1879- 1883.
28. Susmita, S., Bhowmick, A.K., 2004. Preparation and properties of nanocomposites based on acrylonitrile-butadiene rubber, styrene-butadiene rubber, and polybutadiene rubber. J. Polym. Sci. Part B: Polym. Phys. 42, 1573–1585.